

Manuscript version: Author's Accepted Manuscript

The version presented in WRAP is the author's accepted manuscript and may differ from the published version or Version of Record.

Persistent WRAP URL:

<http://wrap.warwick.ac.uk/110799>

How to cite:

Please refer to published version for the most recent bibliographic citation information. If a published version is known of, the repository item page linked to above, will contain details on accessing it.

Copyright and reuse:

The Warwick Research Archive Portal (WRAP) makes this work by researchers of the University of Warwick available open access under the following conditions.

Copyright © and all moral rights to the version of the paper presented here belong to the individual author(s) and/or other copyright owners. To the extent reasonable and practicable the material made available in WRAP has been checked for eligibility before being made available.

Copies of full items can be used for personal research or study, educational, or not-for-profit purposes without prior permission or charge. Provided that the authors, title and full bibliographic details are credited, a hyperlink and/or URL is given for the original metadata page and the content is not changed in any way.

Publisher's statement:

Please refer to the repository item page, publisher's statement section, for further information.

For more information, please contact the WRAP Team at: wrap@warwick.ac.uk.

Coupling Electron Capture Dissociation and the modified Kendrick mass defect for sequencing of a poly(2-ethyl-2-oxazoline) polymer

Tomos E. Morgan¹, Sean H. Ellacott¹, Christopher A. Wootton¹, Mark P. Barrow¹, Anthony W. T. Bristow², Sebastien Perrier¹, Peter B. O'Connor¹

¹Department of Chemistry, University of Warwick, Coventry, Midlands, CV4 7AL, UK.

²AstraZeneca, Macclesfield, Cheshire, SK10 2NA, UK.

ABSTRACT: With increasing focus on the structural elucidation of polymers, advanced tandem mass spectrometry techniques will play a crucial role in the characterization of these compounds. In this contribution, synthesis and analysis of methyl initiated and xanthate terminated poly(2-ethyl-2-oxazoline) using Fourier transform ion cyclotron resonance (FT-ICR) mass spectrometry was achieved. Electron capture dissociation (ECD) produced full end group characterization as well as back bone fragmentation including complete sequence coverage of the polymer. A method of fragment ion characterization is also presented with the use of the high resolution modified Kendrick mass defect plots as a means of grouping fragments from the same fragmentation pathways together. This type of data processing is applicable to all tandem mass spectrometry techniques for polymer analysis but is made more effective with high mass accuracy methods. ECD FT-ICR MS demonstrates its promising role as a structural characterization technique for polyoxazoline species.

Polyoxazolines have recently gained interest as an alternative to poly(ethylene glycol) (PEG) based conjugate species for drug delivery, due to their biological compatibility and in particular their stealth behavior *in vivo*.^{1,2} The use of polyoxazolines over PEG can be justified by a decrease in immunogenicity and because of the potential for better synthetic control and more structural diversity.³⁻⁵ Properties of polyoxazolines are related to their chemical composition, size, and initiating and terminating end groups.⁶ With increasing complexity, there has been a shift in focus on the analysis of the structure of polyoxazolines by tandem mass spectrometry.⁷⁻⁹

Ultra-high resolution mass spectrometry techniques such as Fourier transform ion cyclotron resonance mass spectrometry (FT-ICR MS) can provide fragmentation analysis of polymeric species to determine their structure. Electrospray ionization (ESI) as a means to analyze polyoxazolines has been well established,^{10,11} and multiply charged species are produced which allows the use of electron capture methods.¹²

The use of electron capture dissociation (ECD) fragmentation is limited in the analysis of polymers,^{8,13-15} although ECD analysis of polymeric excipients has been carried out successfully.^{16,17} The N-C α bond adjacent to the amide group is broken when ECD fragmentation occurs in peptides and proteins,¹⁸ making the repeating amide unit within a polyoxazoline a promising target for fragmentation analysis.

The non-selective fragmentation provided by ECD allows much more predictable fragmentation pathways to be present than that of other methods, such as collision-induced/activated dissociation (CID/CAD).

As ECD is a radical-based rather than ergodic technique, the fragmentation coverage is less affected by the presence of particularly weak covalent bonds in the molecule.¹⁹ Analysis of polymers by CID regularly shows the polymer backbone “unzipping” through a series of rearrangements.²⁰ When the polymer is capable of rearrangements allowing monomer release from the major species, then it is common to see near complete backbone fragmentation coverage.²¹⁻²⁴ There are other examples of radicals being produced as part of the ionization process initiating fragmentation down the polymer backbone as part of a radical reaction.²⁵⁻²⁷ CID analysis of polyoxazoline species has often been based on the CID dissociation voltages used to produce fragmentation.^{28,29} CID dissociation measurement varies with internal energy deposition differences between instruments, and is often highly reliant on the strength of bonds within the polymer end groups, as they may fragment before elucidation of the complete polymer chain itself.

Kendrick mass defect (KMD) analysis is used to characterise complex petroleum spectra³⁰ by normalising the mass defect to the CH₂ group, the most common repeating unit within these samples.³¹ Modifying the masses to the homologous series helps simplify complex spectra by grouping measured ions into classes based on their heteroatoms and double bond equivalents. Similarly, modified mass defects are seeing extensive use in the analysis of polymers and complex polymeric samples normalizing the mass defect to that of the homologous series of the monomer instead of CH₂. A “modified” KMD (MKMD)³²⁻³⁷ can visualize high resolution data based on a fractional base unit allowing even more precise assignment with tandem

mass spectrometry,³³ the MKMD groups the fragments based on their end group and adduct variation from different fragmentation pathways.

In this study we report the characterisation of methyl and hydrogen initiated polyoxazolines by ECD fragmentation and how the complex fragmentation patterns can be separated using the MKMD. The use of ECD fragmentation on the polyoxazolines also showed end group fragmentation that allowed complete structural analysis.

Experimental Section:

Synthesis of poly(2-ethyl-2-oxazoline): Microwave synthesis of the poly(2-ethyl-2-oxazoline) was carried out with the reaction capped with the use of ethyl xanthate. A full synthetic methodology is given in the supplementary information.

MS Sample Preparation: The polyoxazoline sample was dissolved into a 99.5% solution of purified water obtained from a Direct-Q3 Ultrapure Water System (Millipore, Lutterworth, United Kingdom) at 20 μM in 0.5% formic acid (Sigma-Aldrich, Dorset, United Kingdom).

FT-ICR MS analysis: All experiments were performed on a 12 T solariX Fourier transform ion cyclotron resonance mass spectrometer (Bruker Daltonik, GmbH, Bremen, Germany) using a nano-electrospray (nESI) ion source in positive ion mode. The ECD was carried out with the use of an indirectly heated hollow cathode with a current set at 1.5 A, with a pulse length of 0.2 s and bias 1.2 eV. All data was recorded using 4 mega-word (2^{22} , 32 bit) transients (1.6777 s) achieving approximately 400 thousand resolving power at m/z 400. All mass spectra were internally calibrated by the intact polymer peaks across the polymer distribution, or by internal calibration of fragment peaks in ECD spectra (peaks used for calibration are marked). The peaks used for internal calibration were cross-checked using both the a and x fragment series. The standard deviation of the calibration was 0.07 ppm and the total standard deviation of the assignments in total was 0.7 ppm, making miss-assignment unlikely. The Bruker SNAP algorithm was used for peak picking with the polyoxazoline monomer used as the repeat unit. The Bruker SNAP algorithm matches a calculated isotope distribution adjusted to a repeat unit with increasing mass.³⁸⁻⁴⁰ Adjusting the mass of the fragment to a function of the monomer was carried out by the modified Kendrick mass analysis importing the mass tables into Excel.³⁹ Equations 1-3 shows the calculation of the HRMKMr, the value 100 is the rescaling factor linked to the monomer mass unit of the homologous series.³³ The round function is to the nearest integer, up or down. The charge, z is determined by the SNAP peak picking algorithm.

$$(1) \frac{m}{z} \times z = m$$

$$(2) \text{HRMKMr} = m \times \frac{\text{Round}\left(\frac{(\text{Exact monomer mass})}{100}\right)}{\left(\frac{(\text{Exact monomer mass})}{100}\right)}$$

$$(3) \text{HRMKMD} = \text{HRMKMr} - \text{Round}(\text{HRMKMr})$$

Equation 1-3: Calculation of the neutral mass, the high-resolution Kendrick mass (HRMKMr), and calculation of the high-resolution Kendrick mass defect (HRMKMD).

Results and Discussion: nano-Electrospray MS analysis, presented in Figure 1, of the polyoxazoline polymer species produced a rich spectrum due to the inherent dispersity of the polymer and multiple charge states produced. The use of the nESI device under acidified conditions produced mainly protonated ions as well as low levels of mono- and di-sodiated adduct ions. The visible charge states were assigned to protonated 2+ (blue rectangles) and 3+ (blue triangles) methyl initiated polyoxazoline ions. There was also a 4+ protonated species present of a much lower intensity than the other charge and adduct species. The higher mass polymer chains showed a higher average charge state than smaller chains as their increased size stabilizes more charge. The spacing between main peaks corresponds to that of the monomer repeat unit as expected. The use of the Bruker SNAP algorithm brings a significant advantage in mass accuracy, the peak picking is based on the entire isotope envelope which is shifted with a repeat unit as the mass increases. Peak picking based on a repeat unit is especially suited to polymer analysis as the use of an average repeat unit can be avoided. This analysis also showed the presence of a low-level hydrogen initiated by-product of the synthesis process.⁴¹ The most abundant ion of the hydrogen initiated by-product was the triply protonated species.

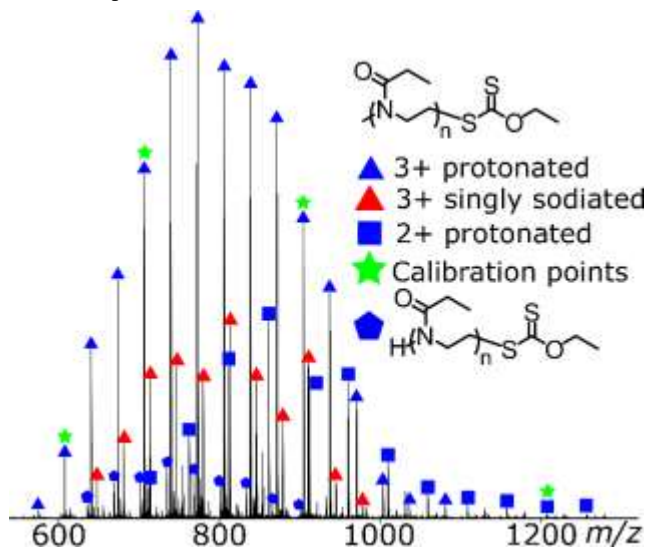


Figure 1. nESI Mass spectrum of the polyoxazoline species showing multiple charge states and the dispersity of the polymer.

Isolation of the protonated methyl initiated 3+ ion at m/z 739.81971 ($n=21$) and the protonated hydrogen initiated 3+ ion at m/z 834.21559 ($n=24$) was carried out separately by both front-end quadrupole isolation and multi-CHEF⁴² in-cell isolation to ensure clean isolation from the rest of the ions. During ECD the ions are held within a close orbit and bathed in low energy fragmentation electrons (cathode voltage 1.2 eV). Figure 2 presents the ECD spectra for the two isolated species.

The ECD event produces an odd electron charge reduced radical cation species which can then follow numerous fragmentation pathways. Common fragmentations observed were neutral losses from the charge capture species as well as backbone fragmentation across the polymer. The ECD spectra of both isolated species show two major fragmentation series, assigned to fragmentation along the polymer backbone, mainly *a* and *x* fragments (defined in figure 3). All *a* and *x* fragments contain an end group, either the initiating methyl or hydrogen, or the terminating xanthate group, and then a varying number of monomer repeat units, dictated by where in the polymer backbone the fragmentation took place. Both the *a* and the *x* fragmentation form a stable imidic end group.

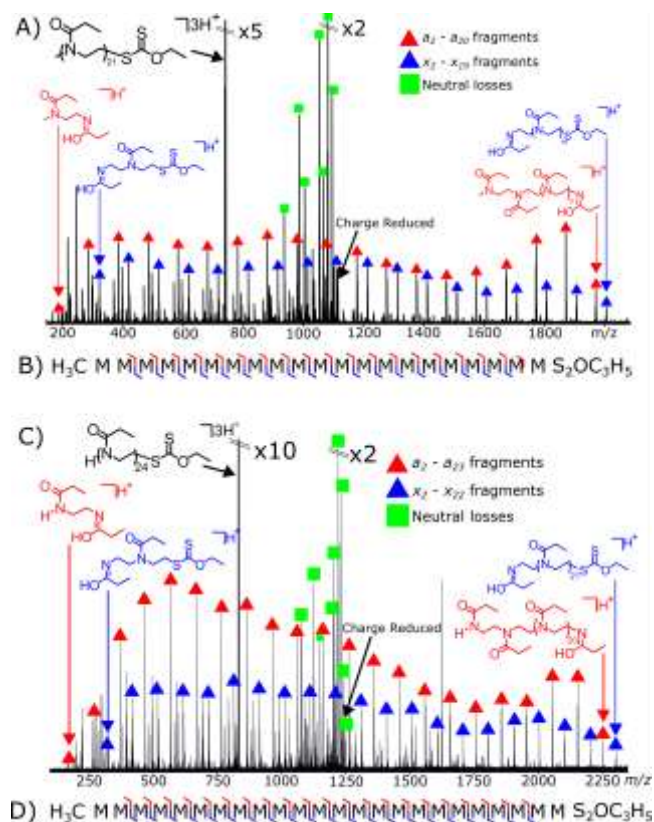


Figure 2. A) and C) ECD spectra of methyl initiated, and hydrogen initiated polyoxazoline respectively with fragmentation maps B) and D), showing clear fragmentation ladders for the 2 key fragment types (marked with red (*a*) and blue (*x*) triangles), along with neutral losses indicating end groups (green squares). Intensity of ions outside of the represented range are marked with a multiplication factor of “x10, x5, and x2”.

The *a* fragmentation series of the methyl initiated polyoxazoline was first observed at m/z 187.14399 this contains the methyl end group and two monomer units (a_2 , 0.61 ppm). This fragmentation series contains 18 monomer spaced fragments ending with m/z 1970.37582 (a_{20} , 0.13 ppm). As the series starts with two monomer units and has a further 18 monomer spaced fragments remaining mass constitutes the terminating xanthate group and a monomer unit. The last fragment in this series would be loss of

an ethyl functionalized xanthate group, which is unlikely to occur as it would produce a singly charged, large polymer ion and a charged xanthate group. The xanthate containing series starts at mass m/z 321.13011 (x_2 , -0.00 ppm) containing the xanthate group and two monomer repeat units. A monomer unit fragmentation series follows this ending at m/z 2005.29034 (x_{19} , 1.43 ppm) which leaves the remainder as two monomer units short.

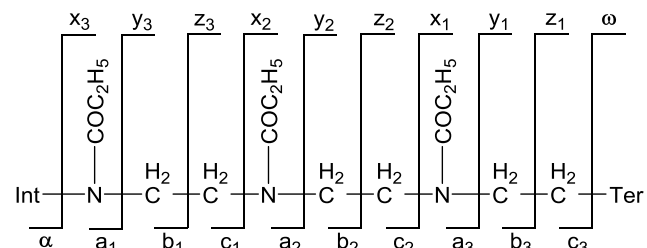


Figure 3. Fragmentation assignments of the polyoxazoline.

The *a* fragmentation series of the hydrogen initiated polyoxazoline starts at mass m/z 173.12845 (a_2 , -0.02 ppm) and the series is monomer spaced to mass m/z 2253.56340 (a_{23} , -0.76 ppm), leaves on monomer and the terminating xanthate group. The *x* fragmentation series starts with the terminating xanthate and two monomer unit m/z 321.13007 (x_2 , -0.13 ppm) and has a total of 19 monomer spaced fragments ending at mass m/z 2302.43950 (x_{22} , -0.20 ppm). As the terminating xanthate group was identical between the methyl and hydrogen initiated polyoxazolines the *x* series fragmentation was also identical.

As a radical directed MS/MS technique, rather than a slow heating process like CAD or IRMPD, ECD produced an evenly distributed fragment coverage of the parent species (Figure 2). Over fragmentation of polymeric species is frequently observed in slow heating processes due to the frequent occurrence and homogeneity of lower energy bonds broken, leading to abundant low m/z fragments. However, ECD produced fragments of relatively even intensity across the entire polymer backbone and complete coverage of the target species. The charge reduced species of both polyoxazolines showed significant neutral losses indicative of the polymer end group chemistry. The charge reduced species of the methyl initiated polyoxazoline $[Me(Mon)_{21}Xan]H_3^{2+}$ (m/z 1109.22564, -0.7 ppm) and the hydrogen initiated polyoxazoline $[H(Mon)_{24}Xan]H_3^{2+}$ were both at much lower intensities than the resulting fragments. The low intensities observed suggests the electron capture species is less able to stabilize the radical, contrasting to peptide/protein ECD where the charge reduced species is usually of a higher intensity than the ECD fragments.

Figure 4, below, summarizes the neutral/radical losses from the charge reduced species (marked with *) of the methyl and hydrogen initiated polyoxazoline, from very similar fragmentation pathways. Fragments from the charge reduced state were often indicative of the functional groups. Many fragments observed from the charge reduced species are based on fragmentation from the α -carbon bond to the amide group, and there is also significant fragmentation of the xanthate groups. The doubly

charged ion observed at m/z 1102.21816 corresponding to the loss of a methyl radical of the initiating group (α , -0.2 ppm) from the charge reduced species. Fragments observed at m/z 1052.36800 showed loss of the methyl group and a repeating monomer unit (a , -0.14 ppm). Elucidation of the xanthate group occurred at two points, with the fragmentation of the C-S bond, m/z 1065.22677 (-0.25 ppm) as well as loss of the ethyl functionalized xanthate end group to produce the fragment at m/z 1035.22512 (y , -0.22 ppm). The presence of these neutral losses from the charge capture species allows precise end group determination of the polymer species. The peak at m/z 1081.21299 can be assigned to a fragmentation of the amide bond itself. This is not a common pathway within ECD fragmentation of peptides but has been documented based on either a loss through secondary fragmentation or due to the nitrogen of the amide itself being protonated or from other ergodic pathways caused by residual collisional activation or the release of coulombic strain.⁴³

Overall, the ECD mass spectra for both molecules shows a rich coverage of backbone and end group fragmentation. Either through a and x fragmentation resulting in a 1+ backbone fragmentation series or through neutral loss from the charge capture species resulting in end group characterization. A large proportion of the fragments observed resulted from a limited number of fragmentation pathways but with a different number of monomer repeat unit. The simplest examples of this is the presence of a and x fragmentation pathways that contain the initiating or terminating end group and the imidic acid formed by the fragmentation itself and then a series of monomer repeat units that all form part of the fragmentation series but are from the same pathway. Grouping fragments as a function of their mass in a way which removes any variation due to difference in monomer number meaning that fragments from the same pathway and end groups can be readily grouped together.

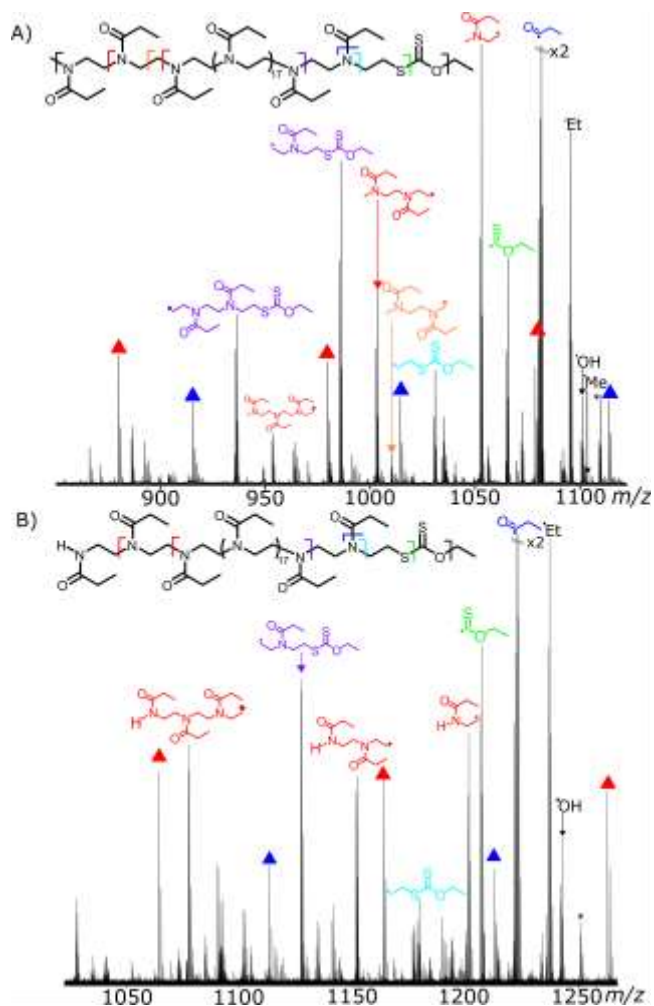


Figure 4. A) methylated polyoxazoline and B) hydrogen initiated polyoxazoline neutral losses showing end group losses and end groups with multiples of monomer units lost, indicating the terminal polymer chemistry.

SNAP peak picking inherently provides accurate charge state information required for isotope matching, and using this charge allows a neutral mass to be calculated easily. For the MKMD analysis, the charge carriers were not corrected for as this could lead to the potential loss of information, and subsequently can provide information on adduct influence of the various fragmentation process. Rescaling the MKMD value to the high-resolution MKMD value means there is a greater separation in the MKMD diagram compared to the non-scaled mass defects of these species. Use of the HRMKMD meant that different pathways, series, and adducts could be easily assigned to a mass defect value, allowing more obvious identification. Fragment chains with the same end group or modification but a varying number of monomer units were present as evenly spaced horizontal lines (Figure 5).

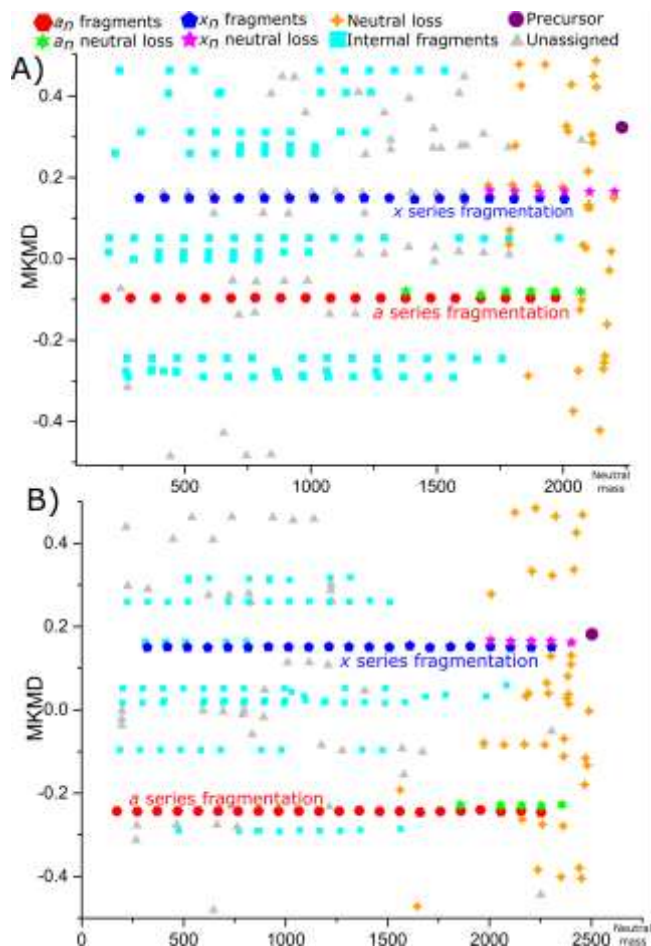


Figure 5. A) The methyl initiated and B) hydrogen initiated fragmentation spectra of the polyoxazoline represented as a modified Kendrick mass defect plot. The different fragmentation series are labeled in different colors.

The presence of horizontal lines allowed rapid assignment of the fragmentation. Spacing in the y dimension is due to presence of atoms that are not part of the monomer unit and the x dimension spacing is in overall mass. Almost all the spacing present between points in the x dimension of the same MKMD value is that of a monomer mass unit. The rescaled MKMD plot showed the two major ladders as along horizontal lines moving through the length of the polymer chain and therefore the mass axis of the MKMD plot. There were also several smaller fragmentation series that were present, spread through numerous MKMD values. As fragments in the same series will have the same repeating composition the end group, adduct, and fragmentation will be constant, allowing grouping of the whole series. The precursor (red) is present at the highest mass in the MKMD plot, as the plot has been charge corrected.

For the methyl initiated polyoxazoline, the fragmentation series at MKMD value of -0.096 shown in purple contains the *a* fragmented series discussed above. The MKMD value that has been assigned for this fragmentation is based on the presence of the methyl end group and the protonation of the fragment. As the MKMD value is based purely on deviation from the homologous series chosen for

the conversion the imidic end group is isobaric to the polyoxazoline repeat, so the methyl group and protonation is all that effects the mass defect. The fragments that are present as purple squares along the same MKMD value are the equally spaced monomer units of that series of fragments. The assignment of the *x* fragmentation series is the dark blue line at 0.149 MKMD. The series as shown by the MKMD value is equal to that found in the original ECD spectra (Figure 2) allowing complete visualization of the fragment series in one line. Above both *a* and *x* series, there are shorter fragment series that have also been highlighted. The fragment series above the *a* fragmentation series is coloured green, the offset in MKMD value is that of a single proton, meaning these are neutral losses that were observed from the charge capture species. The offset is due to the additional proton that is present, and as charge has been accounted for, the spacing remains the same. The presence of the complete *a* and *x* series through both fragmentation and neutral losses shows clear backbone coverage. The *x* series fragmentation line has a neutral loss line above it colored pink, which spans another 2 monomer mass units. Fragmentation of the ethyl functionalized xanthate group meant all of the monomer units were accounted for when the neutral loss is included as part of the fragmentation series. With both *a* and *x* fragmentation accounted for, complete coverage of the polymer was carried out.

The *x* series for the hydrogen initiated polyoxazoline is equal to that of the methyl initiated polyoxazoline as they form the same fragments. The *x* series spans from x_2 to x_{22} at a MKMD value of 0.149. The *x* series also exhibited the presence of the neutral loss series directly above them. The *x* neutral fragment series covers fragmentation from x_{19} – x_{23} . The *a* series fragmentation was at an MKMD value of -0.243, colored pink, this fragmentation series, therefore, varies from the methyl initiated polyoxazoline as the end group was a hydrogen and not a methyl initiator. The fragmentation coverage was very similar, with the fragmentation coverage from a_2 to a_{23} as well as being able to visualize the presence of neutral losses present at a_{20} – a_{23} . These two diagrams combined allow an easy method of visualizing the differences between the fragmentations of the two polymers analyzed.

Internal fragments are seen at other MKMD values (light blue), the larger internal fragment series could be assigned to numerous fragmentation pathways that are shown in the supplementary information. Internal fragmentation pathways offer some analytical use as their relative size suggests an unmodified – unbroken polyoxazoline chain.

Neutral loss fragments, colored orange are shown to have a high deviation away from the precursor in MKMD space due to the large difference in heterogeneity the end groups have compared to the monomer repeat unit. Aliasing of the neutral losses can be seen by the diagonal line moving from -0.5 to 0.5 MKMD values. This effect means that the direct translation from a MKMD value to a mass defect value is more difficult but doesn't affect the overall grouping of ions together.

In conclusion, the use of electron capture dissociation to analyze polyoxazolines has been shown to be effective in achieving end group and primary structure characterization. The fragmentation coverage means that any modification made to polyoxazolines could be accurately characterized using this method of analysis. The loss of the end groups as neutral loss species greatly assisted in the identification of the terminal methyl and xanthate end groups. A significant benefit was also shown by the use of high resolution modified Kendrick mass defect graphs as a way to analyse these complex polymer fragmentation spectra. Separating different fragmentation routes as well as identifying ways to achieve complete backbone characterisation of the polymer due to closely related groups, based off of their MKMD value. This helps to speed up the analysis time as well as being a useful tool for visualization of fragmentation spectra of polymers.

ASSOCIATED CONTENT

Supporting Information

Supporting information, including assignments and NMR and GPC information are included as PDFs as part of this work. The Supporting Information is available free of charge on the ACS Publications website.

AUTHOR INFORMATION

Corresponding Author

* Peter B. O'Connor, University of Warwick, UK. Phone: +44 (0)24 76151008; fax: +44 (0)24 76151009; Email: p.oconnor@warwick.ac.uk;

Author Contributions

All authors have given approval to the final version of the manuscript.

ACKNOWLEDGMENT

This work is funded and supported with an EPSRC CASE AZ studentship (EPSRC EP/N021630/1), the University of Warwick and the Department of Chemistry. Thanks is extended to Yuko Lam, Meng Li, Cookson Chiu, Remy Gavard, Dr. Maria Van Agthoven, and Dr. Diana Catalina Palacio at the University of Warwick for their helpful discussions and input during this work.

REFERENCES

- (1) Pelegri-O'Day, E. M.; Lin, E. W.; Maynard, H. D. *J. Am. Chem. Soc.* **2014**, *136*, 14323-14332.
- (2) Qi, Y.; Chilkoti, A. *Curr. Opin. Chem. Biol.* **2015**, *28*, 181-193.
- (3) Hartlieb, M.; Floyd, T.; Cook, A. B.; Sanchez-Cano, C.; Catrouillet, S.; Burns, J. A.; Perrier, S. *Polym. Chem.* **2017**, *8*, 2041-2054.
- (4) Rudolph, T.; von der Luhe, M.; Hartlieb, M.; Norsic, S.; Schubert, U. S.; Boisson, C.; D'Agosto, F.; Schacher, F. H. *ACS Nano* **2015**, *9*, 10085-10098.
- (5) Dworak, A.; Trzebicka, B.; Kowalczyk, A.; Tsvetanov, C.; Rangelov, S. *Polimery* **2014**, *59*, 88-94.
- (6) Viegas, T. X.; Bentley, M. D.; Harris, J. M.; Fang, Z.; Yoon, K.; Dizman, B.; Weimer, R.; Mero, A.; Pasut, G.; Veronese, F. M. *Bioconjug. Chem.* **2011**, *22*, 976-986.

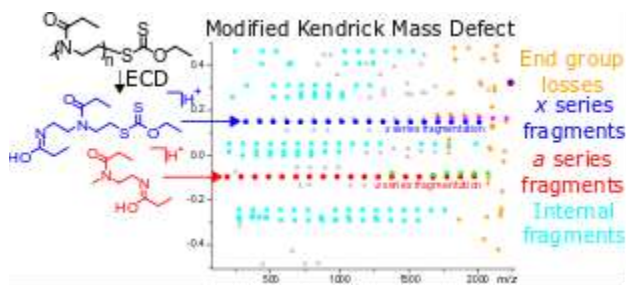
- (7) Crotty, S.; Gerislioglu, S.; Endres, K. J.; Wesdemiotis, C.; Schubert, U. S. *Anal. Chim. Acta.* **2016**, *932*, 1-21.
- (8) Hart-Smith, G. *Anal. Chim. Acta.* **2014**, *808*, 44-55.
- (9) Altuntaş, E.; Schubert, U. S. *Anal. Chim. Acta.* **2014**, *808*, 56-69.
- (10) Altuntaş, E.; Krieg, A.; Baumgaertel, A.; Crecelius, A. C.; Schubert, U. S. *J. Polym. Sci., Part A: Polym. Chem.* **2013**, *51*, 1595-1605.
- (11) Altuntaş, E.; Weber, C.; Kempe, K.; Schubert, U. S. *European Polymer Journal* **2013**, *49*, 2172-2185.
- (12) Yamashita, M.; Fenn, J. B. *J. Phys. Chem.* **1984**, *88*, 4451-4459.
- (13) Crecelius, A. C.; Baumgaertel, A.; Schubert, U. S. *J. Mass Spectrom.* **2009**, *44*, 1277-1286.
- (14) Josse, T.; De Winter, J.; Dubois, P.; Coulembier, O.; Gerbaux, P.; Memboeuf, A. *Polym. Chem.* **2015**, *6*, 64-69.
- (15) Wesdemiotis, C.; Solak, N.; Polce, M. J.; Dabney, D. E.; Chaicharoen, K.; Katzenmeyer, B. C. *Mass Spectrom. Rev.* **2011**, *30*, 523-559.
- (16) Perez Hurtado, P.; Lam, P. Y.; Kilgour, D.; Bristow, A.; McBride, E.; O'Connor, P. B. *Anal. Chem.* **2012**, *84*, 8579-8586.
- (17) Wei, J.; Bristow, A.; McBride, E.; Kilgour, D.; O'Connor, P. B. *Anal. Chem.* **2014**, *86*, 1567-1574.
- (18) Qi, Y.; Volmer, D. A. *Mass Spectrom. Rev.* **2017**, *36*, 4-15.
- (19) Tureček, F. *J. Am. Chem. Soc.* **2003**, *125*, 5954-5963.
- (20) Baumgaertel, A.; Weber, C.; Knop, K.; Crecelius, A.; Schubert, U. S. *Rapid Commun. Mass Spectrom.* **2009**, *23*, 756-762.
- (21) Giordanengo, R.; Viel, S.; Hidalgo, M.; Allard-Breton, B.; Thevand, A.; Charles, L. *Rapid Commun. Mass Spectrom.* **2010**, *24*, 1941-1947.
- (22) Fouquet, T.; Humbel, S.; Charles, L. *J. Am. Soc. Mass Spectrom.* **2011**, *22*, 649-658.
- (23) Nasioudis, A.; Heeren, R. M.; van Doormalen, I.; de Wijs-Rot, N.; van den Brink, O. F. *J. Am. Soc. Mass Spectrom.* **2011**, *22*, 837-844.
- (24) Weidner, S. M.; Falkenhagen, J.; Knop, K.; Thunemann, A. *Rapid Commun. Mass Spectrom.* **2009**, *23*, 2768-2774.
- (25) Girod, M.; Antoine, R.; Lemoine, J.; Dugourd, P.; Charles, L. *Rapid Commun. Mass Spectrom.* **2011**, *25*, 3259-3266.
- (26) Polce, M. J.; Ocampo, M.; Quirk, R. P.; Wesdemiotis, C. *Anal. Chem.* **2008**, *80*, 347-354.
- (27) Polce, M. J.; Ocampo, M.; Quirk, R. P.; Leigh, A. M.; Wesdemiotis, C. *Anal. Chem.* **2008**, *80*, 355-362.
- (28) Altuntaş, E.; Weber, C.; Schubert, U. S. *Rapid Commun. Mass Spectrom.* **2013**, *27*, 1095-1100.
- (29) Baumgaertel, A.; Scheubert, K.; Pietsch, B.; Kempe, K.; Crecelius, A. C.; Bocker, S.; Schubert, U. S. *Rapid Commun. Mass Spectrom.* **2011**, *25*, 1765-1778.
- (30) Kendrick, E. *Anal. Chem.* **1963**, *35*, 2146-2154.
- (31) Hsu, C. S.; Qian, K.; Chen, Y. C. *Anal. Chim. Acta.* **1992**, *264*, 79-89.
- (32) Qi, Y.; Hempelmann, R.; Volmer, D. A. *Anal. Bioanal. Chem.* **2016**, *408*, 4835-4843.
- (33) Fouquet, T.; Sato, H. *Anal. Chem.* **2017**, *89*, 2682-2686.
- (34) Fouquet, T.; Cody, R. B.; Sato, H. *J. Mass Spectrom.* **2017**, *52*, 618-624.
- (35) Fouquet, T.; Nakamura, S.; Sato, H. *Rapid Commun. Mass Spectrom.* **2016**, *30*, 973-981.
- (36) Fouquet, T.; Shimada, H.; Maeno, K.; Ito, K.; Ozeki, Y.; Kitagawa, S.; Ohtani, H.; Sato, H. *J. Oleo. Sci.* **2017**, *66*, 1061-1072.
- (37) Fouquet, T. N. J.; Cody, R. B.; Ozeki, Y.; Kitagawa, S.; Ohtani, H.; Sato, H. *J. Am. Soc. Mass Spectrom.* **2018**, *29*, 1611-1626.
- (38) Köster, C.; Patent, U. S., US 6188064 B1, United States, 2001.
- (39) Wootton, C. A.; Lam, Y. P. Y.; Willetts, M.; van Agthoven, M. A.; Barrow, M. P.; Sadler, P. J.; PB, O. C. *Analyst* **2017**, *142*, 2029-2037.

(40) Kaur, P.; O'Connor, P. B. *J Am Soc Mass Spectrom* **2006**, *17*, 459-468.

(41) Weber, C.; Becer, R. C.; Baumgaertel, A.; Hoogenboom, R.; Schubert, U. S. *Des. Monomers Polym.* **2012**, *12*, 149-165.

(42) de Koning, L. J.; Nibbering, N. M. M.; van Orden, S. L.; Laukien, F. H. *Int. Jour. Mass Spectrom. Ion Proc.* **1997**, *165*, 209-219.

(43) Cooper, H. J. *J. Am. Soc. Mass Spectrom.* **2005**, *16*, 1932-1940.



SUPPORTING INFORMATION

to

Coupling electron capture dissociation and the modified Kendrick mass defect for sequencing of a poly(2-ethyl-2-oxazoline) polymer

by

Tomos E. Morgan¹, Sean H. Ellacott¹, Christopher A. Wootton¹, Mark P. Barrow¹, Anthony W. T. Bristow², Sebastien Perrier¹, Peter B. O'Connor^{1*}

¹Department of Chemistry, University of Warwick, Coventry, Midlands, CV4 7AL, UK.

²AstraZeneca, Macclesfield, Cheshire, SK10 2NA, UK.

*Corresponding authors: Peter O'Connor p.oconnor@warwick.ac.uk

Contents

Synthesis of poly(2-ethyl-2-oxazoline)	9
Table S 1: MS assignment of the polyoxazoline polymer	10
Table S 2: ECD assignments of <i>a</i> and <i>x</i> series along with internal fragments	14
Table S 3: Potential structure of internal fragments, assignments of monomer units are additions to these chains.	18
Table S 4: Neutral losses from charge reduced species of methyl initiated polyoxazoline.....	19
Table S 5: Hydrogen initiated Full ECD assignments of fragmentation series.....	20
Table S 6: Neutral loss assignments of the hydrogen initiated polyoxazoline from the charge reduced species.	23
Table S 7: Example of HRMKMD values and fragments	24
Isolation Window spectra	25
Figure S 2: ¹ H-NMR spectrum of the polyoxazoline.	26
Figure S 3: SEC characterisation of the described poly-2-ethyloxazoline. Measurement was performed in chloroform with 2% trimethylamine additive, a polystyrene calibration was used as described in the Experimental section.....	27

Synthesis of poly(2-ethyl-2-oxazoline)

Synthesis of poly(2-ethyl-2-oxazoline): 2-ethyl-2-oxazoline (99%, Sigma Aldrich, Dorset, United Kingdom EtOx) was dried over barium oxide and distilled under reduced pressure then kept in a Schlenk flask prior to use. Methyl p-toluenesulfonate (98%, VWR International Ltd., Lutterworth, United Kingdom), MeTos was distilled under reduced pressure and kept under a nitrogen atmosphere.

Potassium ethyl xanthogenae (96%, Sigma Aldrich, Dorset, United Kingdom, potassium ethyl xanthate) Acetonitrile Extra Dry (99.9%+, Fisher Scientific, Acros Organics, Loughborough, United Kingdom) were used as purchased. ¹H NMR spectra were measured using Bruker DPX-400 NMR spectrometer which operated at 400.05 MHz. Size exclusion chromatography (SEC) measurements in chloroform (CHCl₃) were performed using an Agilent 390-LC MDS (Agilent Technologies LDA UK, Cheadle, United Kingdom) with differential refractive index (DRI), viscometry (VS), dual-angle light scatter (LS) and two wavelength UV detectors. The system was equipped with 2 x PLgel Mixed D columns (300 x 7.5 mm, linear operating range between 200 and 400,000 g mol⁻¹) and a PLgel 5 μm guard column (Agilent Technologies LDA UK, Cheadle, United Kingdom). The eluent was CHCl₃ with 2% triethylamine additive. SEC used Polystyrene standards (Agilent Easy Vials (Agilent Technologies LDA UK, Cheadle, United Kingdom) were used for calibration (150-350,000 g mol⁻¹).

Polymerisations of 2-ethyl-2-oxazoline were carried on a Biotage Initiator+ microwave synthesizer (Biotage, Uppsala, Sweden). Dry methyl tosylate (0.186 g, 1 mmol), dry 2-ethyl-2-oxazoline (1.983 g, 20 mmol) and extra dry acetonitrile (2.83 mL) were added to a pre-dried Biotage microwave vial, under a constant flux of nitrogen. The vial was sealed, left to stir for 30 s before being heated at 140 °C for 3 min. After cooling, a 2 mL solution of potassium ethyl xanthate (0.192 g, 1.2 mmol) in extra dry acetonitrile was added with a syringe to the polymer mixture for end-capping of the polymer. The solution was left stirring at room temperature for 48 h. Chloroform (50 mL) was added and the organic phase was washed three times with a saturated solution of sodium hydrogen carbonate, with brine and dried on magnesium sulfate. The polymer was reconstituted in 10 mL of dichloromethane before precipitation in diethyl ether and dried overnight in a vacuum oven at 40 °C (yield 1.44 g).

¹H NMR (400 MHz, CDCl₃) δ ppm: 3.75 – 3.13 (m, 80 H, backbone), 3.10 - 2.92 (m, 3 H, Methyl group (α-end)), 2.54 - 2.13 (m, 40 H, CH₂ side chain), 1.44 (t, 2.4 H, Methyl group (xanthate)), 1.23 – 0.98 (m, 60 H, CH₃ side chain).

SEC (CHCl₃, trimethylamine, PS calibration): $M_n = 2,700 \text{ g mol}^{-1}$, $\bar{D} = 1.13$.

Table S 1: MS assignment of the polyoxazoline polymer

m/z	z	Chemical formula assigned	Formula	error (ppm)	notes
723.94274	2	C69H125N13O14S2H+1Na+1	EGP13H+1Na+1	-1.8	2+ singly sodiated
773.47806	2	C74H134N14O15S2H+1Na+1	EGP14H+1Na+1	-0.24	
823.0112	2	C79H143N15O16S2H+1Na+1	EGP15H+1Na+1	-1.53	
872.54583	2	C84H152N16O17S2H+1Na+1	EGP16H+1Na+1	-0.95	
922.08002	2	C89H161N17O18S2H+1Na+1	EGP17H+1Na+1	-0.92	
971.61459	2	C94H170N18O19S2H+1Na+1	EGP18H+1Na+1	-0.5	
1021.1487					
	5	C99H179N19O20S2H+1Na+1	EGP19H+1Na+1	-0.52	
1070.6845		C104H188N20O21S2H+1Na+			
	3	1	EGP20H+1Na+1	0.97	
1120.2166		C109H197N21O22S2H+1Na+			
	1	1	EGP21H+1Na+1	-0.97	
1169.7522		C114H206N22O23S2H+1Na+			
	4	1	EGP22H+1Na+1	0.29	
1219.2865		C119H215N23O24S2H+1Na+			
	6	1	EGP23H+1Na+1	0.37	
615.05684	3	C89H161N17O18S2H+2Na+1	EGP17H+2Na+1	0.82	3+ singly sodiated
648.07852	3	C94H170N18O19S2H+2Na+1	EGP18H+2Na+1	-0.96	
681.10134	3	C99H179N19O20S2H+2Na+1	EGP19H+2Na+1	-0.89	
		C104H188N20O21S2H+2Na+			
714.12405	3	1	EGP20H+2Na+1	-0.98	
		C114H206N22O23S2H+2Na+			
780.16968	3	1	EGP22H+2Na+1	-0.87	
		C119H215N23O24S2H+2Na+			
813.19231	3	1	EGP23H+2Na+1	-1.05	
		C124H224N24O25S2H+2Na+			
846.21527	3	1	EGP24H+2Na+1	-0.83	
		C129H233N25O26S2H+2Na+			
879.23827	3	1	EGP25H+2Na+1	-0.58	
		C134H242N26O27S2H+2Na+			
912.26021	3	1	EGP26H+2Na+1	-1.5	
		C139H251N27O28S2H+2Na+			
945.28339	3	1	EGP27H+2Na+1	-1.05	
		C144H260N28O29S2H+2Na+			
978.30645	3	1	EGP28H+2Na+1	-0.76	
1044.3522		C154H278N30O31S2H+2Na+			
	5	1	EGP30H+2Na+1	-0.53	
1077.3761		C159H287N31O32S2H+2Na+			
	2	3	1	EGP31H+2Na+1	0.48
					2+ doubly sodiated
784.4685	2	C74H134N14O15S2H+0Na+2	EGP14H+0Na+2	-1.27	
834.00264	2	C79H143N15O16S2H+0Na+2	EGP15H+0Na+2	-1.27	
883.53663	2	C84H152N16O17S2H+0Na+2	EGP16H+0Na+2	-1.45	
933.07071	2	C89H161N17O18S2H+0Na+2	EGP17H+0Na+2	-1.51	

982.60552	2	C94H170N18O19S2H+0Na+2	EGP18H+0Na+2	-0.82	
1032.1398	2	C99H179N19O20S2H+0Na+2	EGP19H+0Na+2	-0.71	
1081.6734		C104H188N20O21S2H+0Na+			
1	2	2	EGP20H+0Na+2	-1.23	
1131.2078		C109H197N21O22S2H+0Na+			
3	2	2	EGP21H+0Na+2	-0.98	
1180.7415		C114H206N22O23S2H+0Na+			
7	2	2	EGP22H+0Na+2	-1.34	
1230.2766		C119H215N23O24S2H+0Na+			
3	2	2	EGP23H+0Na+2	-0.59	
					3+ doubly sodi- ated
655.40628	3	C94H170N18O19S2H+1Na+2	EGP18H+1Na+2	-0.55	
688.42862	3	C99H179N19O20S2H+1Na+2	EGP19H+1Na+2	-1.2	
		C104H188N20O21S2H+1Na+			
721.45124	3	2	EGP20H+1Na+2	-1.4	
		C109H197N21O22S2H+1Na+			
754.47424	3	2	EGP21H+1Na+2	-1.08	
		C114H206N22O23S2H+1Na+			
787.49692	3	2	EGP22H+1Na+2	-1.19	
		C119H215N23O24S2H+1Na+			
820.51975	3	2	EGP23H+1Na+2	-1.11	
		C124H224N24O25S2H+1Na+			
853.54251	3	2	EGP24H+1Na+2	-1.12	
		C134H242N26O27S2H+1Na+			
919.58793	3	2	EGP26H+1Na+2	-1.25	
					Hydrogen initi- ated 2+ proto- nated
606.87669	2	C58H105N11O12S2H+2Na+0	EGP11H+2Na+0	0.22	
656.41077	2	C63H114N12O13S2H+2Na+0	EGP12H+2Na+0	0.01	
755.47818	2	C73H132N14O15S2H+2Na+0	EGP14H+2Na+0	-1.32	
854.54706	2	C83H150N16O17S2H+2Na+0	EGP16H+2Na+0	-0.62	
953.61554	2	C93H168N18O19S2H+2Na+0	EGP18H+2Na+0	-0.49	
1003.1494	2	C98H177N19O20S2H+2Na+0	EGP19H+2Na+0	-0.81	
1052.6845		C103H186N20O21S2H+2Na+			
3	2	0	EGP20H+2Na+0	0.11	
1151.7524		C113H204N22O23S2H+2Na+			
5	2	0	EGP22H+2Na+0	-0.33	
1201.2879		C118H213N23O24S2H+2Na+			
4	2	0	EGP23H+2Na+0	0.75	
					Hydrogen initi- ated 3+ proto- nated
603.05681	3	C88H159N17O18S2H+3Na+0	EGP17H+3Na+0	-0.24	
636.07941	3	C93H168N18O19S2H+3Na+0	EGP18H+3Na+0	-0.55	
669.10206	3	C98H177N19O20S2H+3Na+0	EGP19H+3Na+0	-0.76	
		C103H186N20O21S2H+3Na+			
702.12487	3	0	EGP20H+3Na+0	-0.71	
		C108H195N21O22S2H+3Na+			
735.1474	3	0	EGP21H+3Na+0	-1.06	

768.1703	3	0	C113H204N22O23S2H+3Na+	EGP22H+3Na+0	-0.89	
801.19269	3	0	C118H213N23O24S2H+3Na+	EGP23H+3Na+0	-1.37	
834.21588	3	0	C123H222N24O25S2H+3Na+	EGP24H+3Na+0	-0.85	
867.23888	3	0	C128H231N25O26S2H+3Na+	EGP25H+3Na+0	-0.59	
900.26204	3	0	C133H240N26O27S2H+3Na+	EGP26H+3Na+0	-0.18	
933.28417	3	0	C138H249N27O28S2H+3Na+	EGP27H+3Na+0	-0.89	
966.30747	3	0	C143H258N28O29S2H+3Na+	EGP28H+3Na+0	-0.35	
613.88422	2		C59H107N11O12S2H+2Na+0	EGP11H+2Na+0	-0.26	2+ protonated
663.41866	2		C64H116N12O13S2H+2Na+0	EGP12H+2Na+0	0.11	
712.95305	2		C69H125N13O14S2H+2Na+0	EGP13H+2Na+0	0.36	
762.48679	2		C74H134N14O15S2H+2Na+0	EGP14H+2Na+0	-0.28	
861.55517	2		C84H152N16O17S2H+2Na+0	EGP16H+2Na+0	-0.29	
911.08964	2		C89H161N17O18S2H+2Na+0	EGP17H+2Na+0	0.02	
960.62319	2		C94H170N18O19S2H+2Na+0	EGP18H+2Na+0	-0.67	
1010.1576	6	2	C99H179N19O20S2H+2Na+0	EGP19H+2Na+0	-0.37	
1059.6923	3	2	C104H188N20O21S2H+2Na+	EGP20H+2Na+0	0.08	
1109.2264	3	2	C109H197N21O22S2H+2Na+	EGP21H+2Na+0	-0.02	
1158.7594	4	2	C114H206N22O23S2H+2Na+	EGP22H+2Na+0	-1.05	
1208.2929	2	0	C119H215N23O24S2H+2Na+	EGP23H+2Na+0	-1.63	
1257.8290	8	2	C124H224N24O25S2H+2Na+	EGP24H+2Na+0	0.01	
574.70604	3		C84H152N16O17S2H+3Na+0	EGP16H+3Na+0	0.01	3+ protonated
607.729	3		C89H161N17O18S2H+3Na+0	EGP17H+3Na+0	0.26	
640.75163	3		C94H170N18O19S2H+3Na+0	EGP18H+3Na+0	-0.02	
673.77447	3		C99H179N19O20S2H+3Na+0	EGP19H+3Na+0	0.03	
706.79707	3	0	C104H188N20O21S2H+3Na+	EGP20H+3Na+0	-0.26	
739.82002	3	0	C109H197N21O22S2H+3Na+	EGP21H+3Na+0	-0.05	
772.84286	3	0	C114H206N22O23S2H+3Na+	EGP22H+3Na+0	-0.01	
805.86578	3	0	C119H215N23O24S2H+3Na+	EGP23H+3Na+0	0.14	
838.88855	3	0	C124H224N24O25S2H+3Na+	EGP24H+3Na+0	0.09	

871.91119	3	0	C129H233N25O26S2H+3Na+	EGP25H+3Na+0	-0.1	
904.93384	3	0	C134H242N26O27S2H+3Na+	EGP26H+3Na+0	-0.27	
937.95656	3	0	C139H251N27O28S2H+3Na+	EGP27H+3Na+0	-0.35	
970.97921	3	0	C144H260N28O29S2H+3Na+	EGP28H+3Na+0	-0.5	
1004.0023	2	3	0	EGP29H+3Na+0	-0.18	
1070.0482	9	3	0	EGP31H+3Na+0	0.17	
1103.0725	8	3	0	EGP32H+3Na+0	1.51	
703.71878	4	0	C139H251N27O28S2H+4Na+	EGP27H+4Na+0	-1	4+ protonated
728.4858	4	0	C144H260N28O29S2H+4Na+	EGP28H+4Na+0	-1.08	
753.25276	4	0	C149H269N29O30S2H+4Na+	EGP29H+4Na+0	-1.24	
778.01942	4	0	C154H278N30O31S2H+4Na+	EGP30H+4Na+0	-1.77	
802.78692	4	0	C159H287N31O32S2H+4Na+	EGP31H+4Na+0	-1.22	
827.55444	4	0	C164H296N32O33S2H+4Na+	EGP32H+4Na+0	-0.68	
852.32099	4	0	C169H305N33O34S2H+4Na+	EGP33H+4Na+0	-1.31	
766.46975	2		C73H132N14O15S2H+1Na+1	EGP14H+1Na+1	-0.88	
865.53879	2		C83H150N16O17S2H+1Na+1	EGP16H+1Na+1	-0.05	
915.07232	2		C88H159N17O18S2H+1Na+1	EGP17H+1Na+1	-0.79	
964.60703	2		C93H168N18O19S2H+1Na+1	EGP18H+1Na+1	-0.23	
				Average		-0.55
				Standard		0.68
				Deviation		

Table S 2: ECD assignments of α and x series along with internal fragments

m/z	charge	Chemical	error	Series
277.10381	1	C11H20N2O2S2H+1	-0.31	Internal
574.30917	1	C26H47N5O5S2H+1	0.06	
673.37769	1	C31H56N6O6S2H+1	0.2	
772.44594	1	C36H65N7O7S2H+1	-0.03	
871.51433	1	C41H74N8O8S2H+1	-0.06	
970.58297	1	C46H83N9O9S2H+1	0.18	
1069.65107	1	C51H92N10O10S2H+1	-0.13	
1168.71994	1	C56H101N11O11S2H+1	0.27	
1267.78864	1	C61H110N12O12S2H+1	0.48	
1366.85692	1	C66H119N13O13S2H+1	0.34	
1465.92348	1	C71H128N14O14S2H+1	-0.94	
1564.99274	1	C76H137N15O15S2H+1	-0.34	
268.20191	1	C14H25N3O2S0H+1	-0.16	Internal
367.27029	1	C19H34N4O3S0H+1	-0.21	
466.33892	1	C24H43N5O4S0H+1	0.3	
862.61142	1	C44H79N9O8S0H+1	-1.18	
1258.88559	1	C64H115N13O12S0H+1	-0.4	
272.19684	1	C13H25N3O3S0H+1	-0.1	Internal
371.26528	1	C18H34N4O4S0H+1	-0.01	
470.33369	1	C23H43N5O5S0H+1	-0.01	
569.40212	1	C28H52N6O6S0H+1	0.02	
668.47053	1	C33H61N7O7S0H+1	0.01	
767.5389	1	C38H70N8O8S0H+1	-0.05	
965.67579	1	C48H88N10O10S0H+1	0.03	
1064.74437	1	C53H97N11O11S0H+1	0.18	
1163.81262	1	C58H106N12O12S0H+1	0.02	
1262.87932	1	C63H115N13O13S0H+1	-1.34	
1361.94956	1	C68H124N14O14S0H+1	0.1	
1461.01617	1	C73H133N15O15S0H+1	-1.14	
1560.08706	1	C78H142N16O16S0H+1	0.52	
1659.15251	1	C83H151N17O17S0H+1	-1.3	
1758.22187	1	C88H160N18O18S0H+1	-0.69	
187.14399	1	C9H18N2O2S0H+1	-0.61	α -series fragments
286.21252	1	C14H27N3O3S0H+1	0.01	
385.28096	1	C19H36N4O4S0H+1	0.07	
484.34935	1	C24H45N5O5S0H+1	0.01	
583.41776	1	C29H54N6O6S0H+1	0	
682.48624	1	C34H63N7O7S0H+1	0.1	
781.55455	1	C39H72N8O8S0H+1	-0.05	
880.62319	1	C44H81N9O9S0H+1	0.21	
979.69159	1	C49H90N10O10S0H+1	0.18	
1078.75997	1	C54H99N11O11S0H+1	0.13	
1177.82824	1	C59H108N12O12S0H+1	0	
1276.89664	1	C64H117N13O13S0H+1	-0.01	
1375.96458	1	C69H126N14O14S0H+1	-0.36	

1475.03329	1	C74H135N15O15S0H+1	-0.13	
1574.10174	1	C79H144N16O16S0H+1	-0.1	
1673.16892	1	C84H153N17O17S0H+1	-0.83	
1772.23795	1	C89H162N18O18S0H+1	-0.44	
1871.306	1	C94H171N19O19S0H+1	-0.61	
1970.37582	1	C99H180N20O20S0H+1	0.13	
688.48482	2	CHNOSH+	0	
837.08491	2	C84H153N17O17S0H+2	-4.64	
886.62253	2	C89H162N18O18S0H+2	-0.53	
936.15684	2	C94H171N19O19S0H+2	-0.39	
985.69105	2	C99H180N20O20S0H+2	-0.37	
1035.22514	2	C104H189N21O21S0H+2	-0.47	
297.20466	1	C15H26N3O3S0H+1	-0.11	Internal
396.2731	1	C20H35N4O4S0H+1	-0.02	
495.34155	1	C25H44N5O5S0H+1	0.06	
594.41006	1	C30H53N6O6S0H+1	0.21	
693.47826	1	C35H62N7O7S0H+1	-0.13	
792.54627	1	C40H71N8O8S0H+1	-0.62	
199.14398	1	C10H18N2O2S0H+1	-0.62	
397.28091	1	C20H36N4O4S0H+1	-0.06	
496.34939	1	C25H45N5O5S0H+1	0.09	
595.41776	1	C30H54N6O6S0H+1	0	
694.48635	1	C35H63N7O7S0H+1	0.25	
793.55479	1	C40H72N8O8S0H+1	0.25	
892.62304	1	C45H81N9O9S0H+1	0.04	
991.69132	1	C50H90N10O10S0H+1	-0.1	
201.15964	1	C10H20N2O2S0H+1	-0.57	Internal
300.22814	1	C15H29N3O3S0H+1	-0.09	
399.29658	1	C20H38N4O4S0H+1	-0.01	
498.36501	1	C25H47N5O5S0H+1	0.03	
597.43347	1	C30H56N6O6S0H+1	0.1	
696.50182	1	C35H65N7O7S0H+1	-0.01	
795.57041	1	C40H74N8O8S0H+1	0.22	
894.63881	1	C45H83N9O9S0H+1	0.18	
993.70692	1	C50H92N10O10S0H+1	-0.15	
1092.77545	1	C55H101N11O11S0H+1	-0.03	
1191.84352	1	C60H110N12O12S0H+1	-0.31	
1290.91315	1	C65H119N13O13S0H+1	0.65	
1588.11791	1	C80H146N16O16S0H+1	0.23	
1687.18495	1	C85H155N17O17S0H+1	-0.6	
1786.25356	1	C90H164N18O18S0H+1	-0.46	
1984.39132	1	C100H182N20O20S0H+1	0.06	
321.13011	1	C13H24N2O3S2H+1	0	x-series
420.19854	1	C18H33N3O4S2H+1	0.04	
519.267	1	C23H42N4O5S2H+1	0.12	
618.33544	1	C28H51N5O6S2H+1	0.14	
717.40375	1	C33H60N6O7S2H+1	-0.02	

816.47225	1	C38H69N7O8S2H+1	0.08	
915.54071	1	C43H78N8O9S2H+1	0.13	
1014.60903	1	C48H87N9O10S2H+1	0.02	
1113.6774	1	C53H96N10O11S2H+1	-0.02	
1212.74625	1	C58H105N11O12S2H+1	0.34	
1311.81443	1	C63H114N12O13S2H+1	0.14	
1410.88015	1	C68H123N13O14S2H+1	-1.78	
1509.95097	1	C73H132N14O15S2H+1	-0.07	
1609.01932	1	C78H141N15O16S2H+1	-0.11	
1708.08733	1	C83H150N16O17S2H+1	-0.34	
1807.15479	1	C88H159N17O18S2H+1	-0.85	
1906.226	1	C93H168N18O19S2H+1	0.66	
2005.29034	1	C98H177N19O20S2H+1	-1.4	
224.15188	1	C12H19N2O2S0H+1	-0.22	Internal
521.35717	1	C27H46N5O5S0H+1	0	
620.42574	1	C32H55N6O6S0H+1	0.25	
719.49419	1	C37H64N7O7S0H+1	0.27	
818.5627	1	C42H73N8O8S0H+1	0.35	
917.63102	1	C47H82N9O9S0H+1	0.21	
1016.69921	1	C52H91N10O10S0H+1	-0.03	
326.24384	1	C17H31N3O3S0H+1	0.07	Internal
524.38069	1	C27H49N5O5S0H+1	0.08	
623.449	1	C32H58N6O6S0H+1	-0.1	
722.51725	1	C37H67N7O7S0H+1	-0.31	
821.58578	1	C42H76N8O8S0H+1	-0.13	
920.6546	1	C47H85N9O9S0H+1	0.32	
1118.7916	1	C57H103N11O11S0H+1	0.42	
1217.85926	1	C62H112N12O12S0H+1	-0.23	
436.30439	1	C23H39N4O4S0H+1	-0.04	
634.44048	1	C33H57N6O6S0H+1	-1.19	
242.18625	1	C12H23N3O2S0H+1	-0.22	Internal
440.32316	1	C22H41N5O4S0H+1	0.07	
539.3915	1	C27H50N6O5S0H+1	-0.08	
1034.73411	1	C52H95N11O10S0H+1	0.48	
1133.80179	1	C57H104N12O11S0H+1	-0.21	
1232.87041	1	C62H113N13O12S0H+1	-0.03	
1331.93899	1	C67H122N14O13S0H+1	0.1	
1431.00768	1	C72H131N15O14S0H+1	0.29	
1530.07521	1	C77H140N16O15S0H+1	-0.31	
			Average	
			Standard	-0.12
			Deviation	
				0.41

Table S 3: Potential structure of internal fragments, assignments of monomer units are additions to these chains.

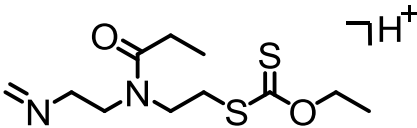
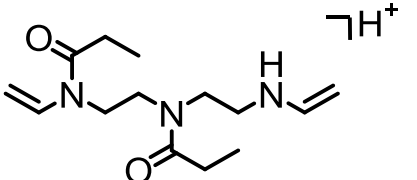
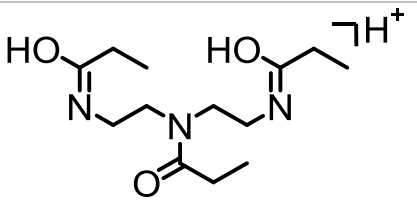
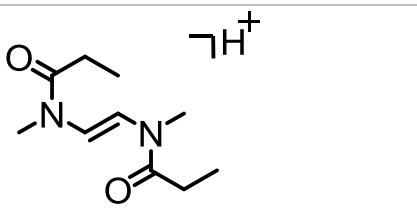
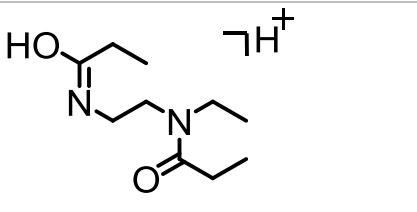
Structure	HRMKMD Value	Fragment mass	Error (ppm)
	-0.290	277.10381	-0.31
	-0.276	268.20191	-0.16
	-0.244	272.19684	-0.10
$C_{15}H_{26}N_3O_3^+$	0.000	297.20466	-0.11
	0.017	199.14398	-0.62
	0.051	201.15964	-0.57

Table S 4: Neutral losses from charge reduced species of methyl initiated polyoxazoline

<i>m/z</i>	Mass	Chemical composition	Loss	$\Delta m/ppm$
1102.21816	2204.43632	C ₁₀₈ H ₁₉₇ N ₂₁ O ₂₂ S ₂	CH ₃	-0.17
1100.72468	2201.44932	C ₁₀₉ H ₁₉₈ N ₂₁ O ₂₁ S ₂	OH	-0.13
1095.21026	2190.42050	C ₁₀₇ H ₁₉₅ N ₂₁ O ₂₂ S ₂	CH ₃ CH ₂	-0.25
1081.21301	2162.42598	C ₁₀₆ H ₁₉₅ N ₂₁ O ₂₁ S ₂	C ₃ H ₅ O	-0.07
1065.22678	2130.45354	C ₁₀₆ H ₁₉₅ N ₂₁ O ₂₁ S ₁	C ₃ H ₅ OS	-0.25
1052.68401	2105.36800	C ₁₀₃ H ₁₈₈ N ₂₀ O ₂₁ S ₂	C ₆ H ₁₂ NO	-0.14
1035.22514	2070.45024	C ₁₀₄ H ₁₉₁ N ₂₁ O ₂₁	C ₅ H ₉ OS ₂	-0.22
1010.15772	2020.31542	C ₉₉ H ₁₈₁ N ₁₉ O ₂₀ S ₂	C ₁₀ H ₁₉ N ₂ O ₂	-0.05
1003.14983	2006.29964	C ₉₈ H ₁₇₉ N ₁₉ O ₂₀ S ₂	C ₁₁ H ₂₁ N ₂ O ₂	-0.12
985.69105	1971.38206	C ₉₉ H ₁₈₂ N ₂₀ O ₂₀	C ₁₀ H ₁₈ NO ₂ S ₂	-0.11
			Average	-0.20
			Standard Deviation	0.18

Table S 5: Hydrogen initiated Full ECD assignments of fragmentation series

m/z	z	Formula	error	Fragmentation
272.19692	1	C8H16N2O2S0H+1	-0.02	α -series fragmentation
371.26529	1	C13H25N3O3S0H+1	0.19	
470.33368	1	C18H34N4O4S0H+1	0.02	
569.40202	1	C23H43N5O5S0H+1	-0.03	
668.47052	1	C28H52N6O6S0H+1	-0.16	
767.53889	1	C33H61N7O7S0H+1	-0.01	
866.60772	1	C38H70N8O8S0H+1	-0.06	
965.67589	1	C43H79N9O9S0H+1	0.43	
1064.74423	1	C48H88N10O10S0H+1	0.13	
1163.81253	1	C53H97N11O11S0H+1	0.05	
1262.88104	1	C58H106N12O12S0H+1	-0.05	
1361.95028	1	C63H115N13O13S0H+1	0.03	
1461.01763	1	C68H124N14O14S0H+1	0.63	
1560.086	1	C73H133N15O15S0H+1	-0.14	
1659.15248	1	C78H142N16O16S0H+1	-0.16	
1758.22349	1	C83H151N17O17S0H+1	-1.32	
1857.29534	1	C88H160N18O18S0H+1	0.23	
1956.36348	1	C93H169N19O19S0H+1	2.07	
2055.42845	1	C98H178N20O20S0H+1	1.83	
2154.49923	1	C103H187N21O21S0H+1	0.06	
2253.56343	1	C108H196N22O22S0H+1	1.16	
196.12062	1	C113H205N23O23S0H+1	-0.76	
298.21253	1	C10H18N2O2S0H+1	-0.07	internal
397.28089	1	C15H27N3O3S0H+1	0.04	
595.41781	1	C20H36N4O4S0H+1	-0.11	
694.48697	1	C30H54N6O6S0H+1	0.08	
793.55477	1	C35H63N7O7S0H+1	1.15	
892.62397	1	C40H72N8O8S0H+1	0.23	
991.69105	1	C45H81N9O9S0H+1	1.08	
1189.82981	1	C50H90N10O10S0H+1	-0.37	
1288.89688	1	C60H108N12O12S0H+1	1.32	
1387.9668	1	C65H117N13O13S0H+1	0.17	
1487.03275	1	C70H126N14O14S0H+1	1.25	
1586.10303	1	C75H135N15O15S0H+1	-0.49	
404.22132	1	C80H144N16O16S0H+1	0.71	
300.22819	1	C10H20N2O2S0H+1	-0.02	internal
399.29659	1	C15H29N3O3S0H+1	0.07	
498.3649	1	C20H38N4O4S0H+1	0.02	
597.43344	1	C25H47N5O5S0H+1	-0.19	
696.5018	1	C30H56N6O6S0H+1	0.05	
795.57035	1	C35H65N7O7S0H+1	-0.03	
993.70744	1	C40H74N8O8S0H+1	0.14	
1290.91343	1	C50H92N10O10S0H+1	0.38	
420.19845	1	C13H24N2O3S2H+1	-0.13	x-series fragmentation
519.26692	1	C18H33N3O4S2H+1	-0.18	

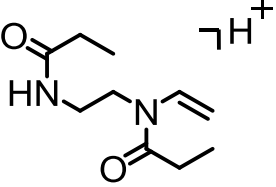
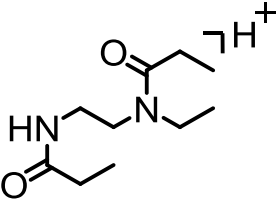
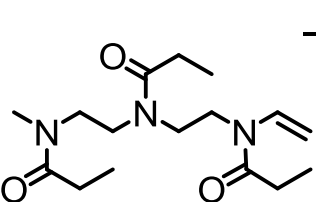
618.33495	1	C23H42N4O5S2H+1	-0.04	
717.40375	1	C28H51N5O6S2H+1	-0.65	
816.47092	1	C33H60N6O7S2H+1	-0.02	
915.54061	1	C38H69N7O8S2H+1	-1.54	
1014.60909	1	C43H78N8O9S2H+1	0.02	
1113.67738	1	C48H87N9O10S2H+1	0.08	
1212.74642	1	C53H96N10O11S2H+1	-0.04	
1311.81434	1	C58H105N11O12S2H+1	0.48	
1410.88324	1	C63H114N12O13S2H+1	0.07	
1509.95028	1	C68H123N13O14S2H+1	0.41	
1609.02168	1	C73H132N14O15S2H+1	-0.53	
1708.08618	1	C78H141N15O16S2H+1	1.36	
1807.15634	1	C83H150N16O17S2H+1	-1.01	
1906.22596	1	C88H159N17O18S2H+1	0.01	
2005.29377	1	C93H168N18O19S2H+1	0.64	
2104.36165	1	C98H177N19O20S2H+1	0.31	
2203.42949	1	C103H186N20O21S2H+1	0.04	
2302.50202	1	C108H195N21O22S2H+1	-0.22	
312.22826	1	C113H204N22O23S2H+1	1.58	
411.29647	1	C16H29N3O3S0H+1	0.29	internal
510.36478	1	C21H38N4O4S0H+1	-0.27	
708.50162	1	C26H47N5O5S0H+1	-0.42	
807.57092	1	C36H65N7O7S0H+1	-0.29	
224.15195	1	C41H74N8O8S0H+1	0.84	
323.22033	1	C12H19N2O2S0H+1	0.09	
422.28889	1	C17H28N3O3S0H+1	-0.04	
521.35735	1	C22H37N4O4S0H+1	0.31	
719.49385	1	C27H46N5O5S0H+1	0.34	
818.56279	1	C37H64N7O7S0H+1	-0.21	
917.631	1	C42H73N8O8S0H+1	0.46	
1016.70036	1	C47H82N9O9S0H+1	0.19	
1115.76915	1	C52H91N10O10S0H+1	1.1	
1214.83526	1	C57H100N11O11S0H+1	1.34	
1313.90418	1	C62H109N12O12S0H+1	-0.67	
1412.97555	1	C67H118N13O13S0H+1	-0.23	
1512.0402	1	C72H127N14O14S0H+1	1.88	
524.38022	1	C77H136N15O15S0H+1	-0.73	
286.21255	1	C9H18N2O2S0H+1	-0.08	internal
385.28095	1	C14H27N3O3S0H+1	0.11	
484.34936	1	C19H36N4O4S0H+1	0.05	
583.41738	1	C24H45N5O5S0H+1	0.03	
682.48623	1	C29H54N6O6S0H+1	-0.65	
880.62309	1	C34H63N7O7S0H+1	0.08	
979.69176	1	C44H81N9O9S0H+1	0.1	
1375.9651	1	C49H90N10O10S0H+1	0.35	
1475.03289	1	C69H126N14O14S0H+1	0.02	
834.21559	3	C74H135N15O15S0H+1	-0.4	

396.27313	2	C123H222N24O25S2H+3	-1.2	
			Average	0.04
			Standard Deviation	0.71

Table S 6: Neutral loss assignments of the hydrogen initiated polyoxazoline from the charge reduced species.

m/z	mass	Chemical Formula	loss	ppm error
1250.82082	2501.64249	C123H221N24O25S2H+3	CH3	-0.61
1242.31712	2484.63921	C123H220N24O24S2H+3	OH	-0.99
1236.80392	2473.61064	C121H217N24O25S2H+3	CH3CH2	-0.1
1222.30363	2444.60791	C120H216N24O24S2H+3	C3H5O	0.84
1206.81998	2413.64366	C120H217N24O24S1H+3	C3H5OS	-0.37
1201.28553	2402.57353	C118H212N23O24S2H+3	C5H10NO	-0.14
1176.8203	2353.64029	C118H213N24O24S0H+3	C5H9OS2	0.13
1151.7508	2303.50512	C113H203N22O23S2H+3	C10H19N2O2	-0.28
1141.300014	2282.60317	C115H208N23O23S0H+3	C8H14NO2S2	-0.01
1127.28462	2254.57187	C113H204N23O23S0H+3	C10H18NO2S2	-0.05
			Average	-0.17
			Standard Deviation	0.57

Table S 7: Example of HRMKMD values and fragments

Structure	HRMKMD Value	Fragment mass	Error (ppm)
	0.0167	199.14409	-0.07
	0.05	201.15975	-0.02
	0.164	312.22826	0.29

Isolation Window spectra

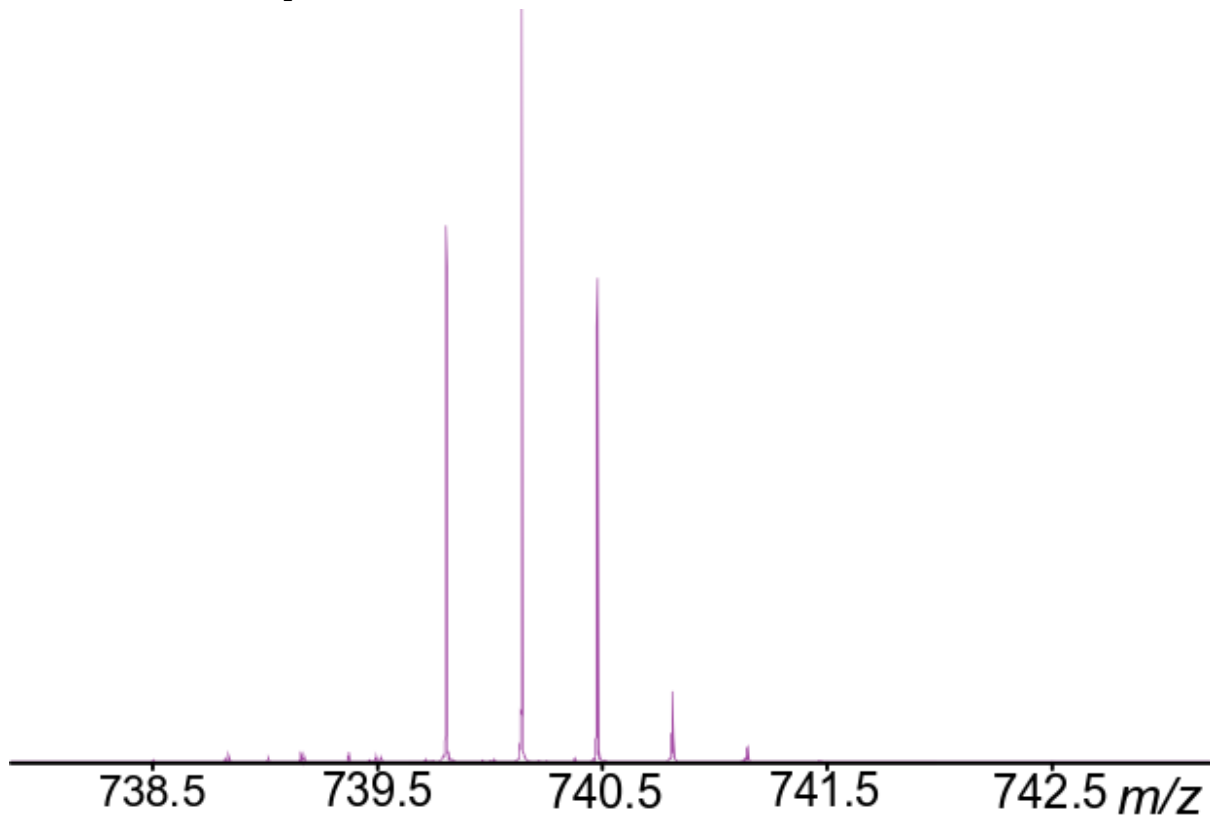


Figure S 1: Isolation window of the methyl initiated polyoxazoline precursor.

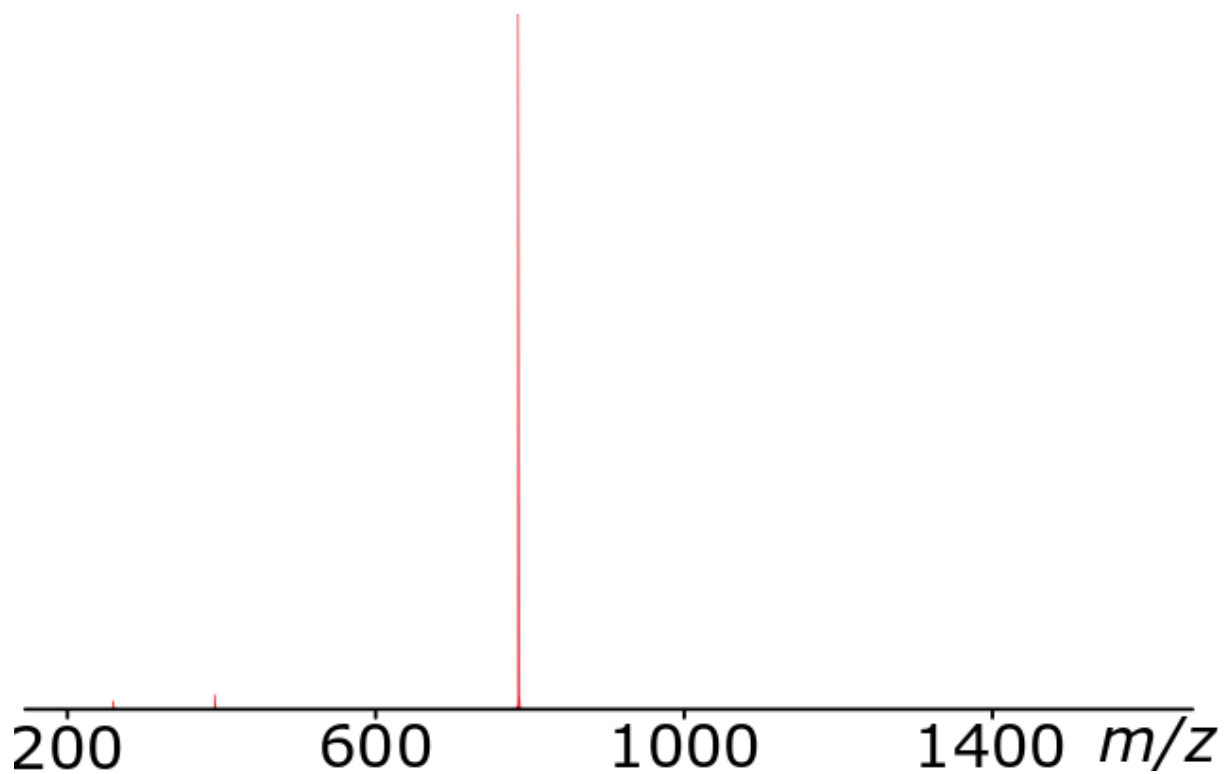


Figure S 2: Full Isolation spectrum of methyl initiated polyoxazoline precursor.

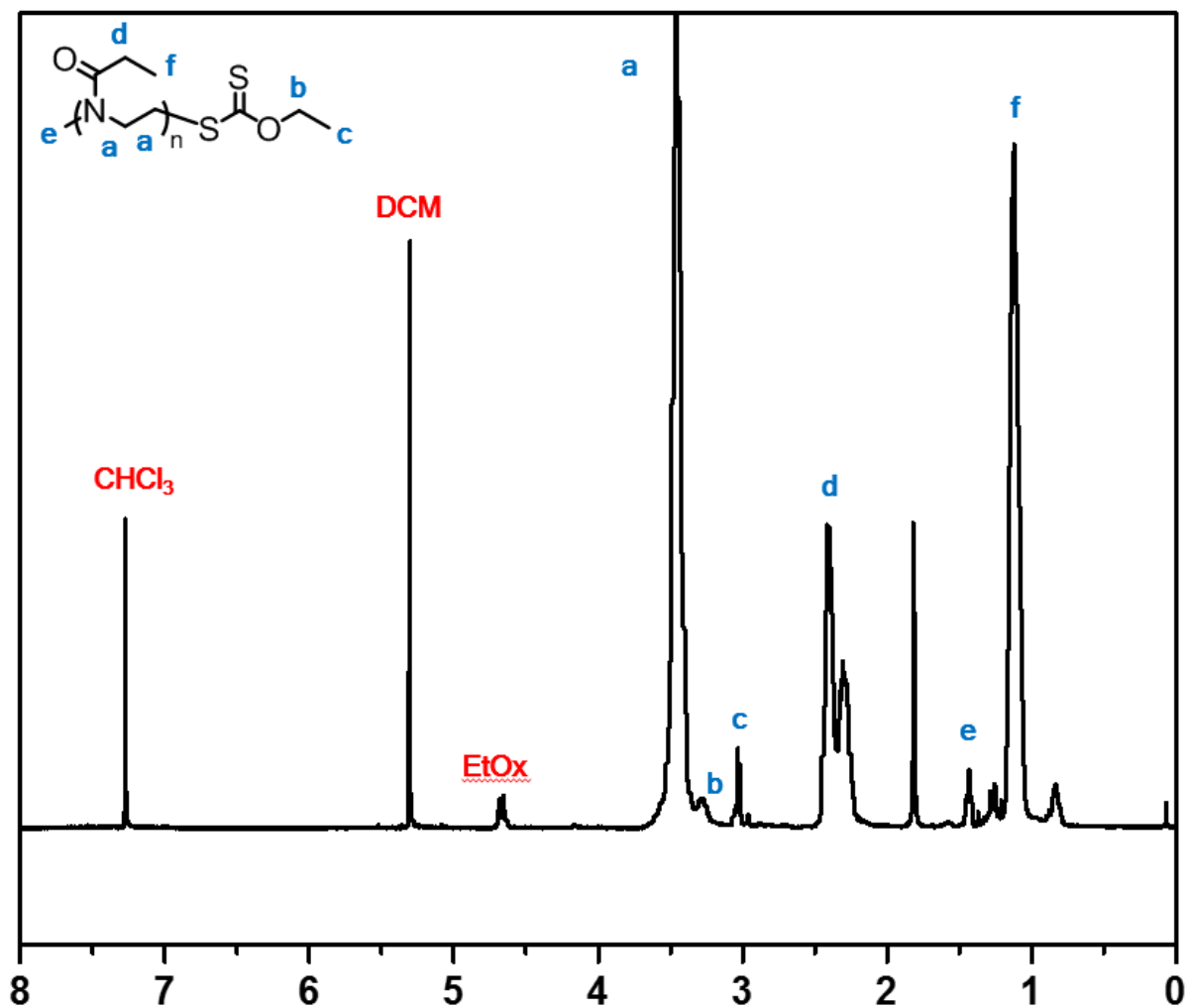


Figure S 3: $^1\text{H-NMR}$ spectrum of the polyoxazoline.

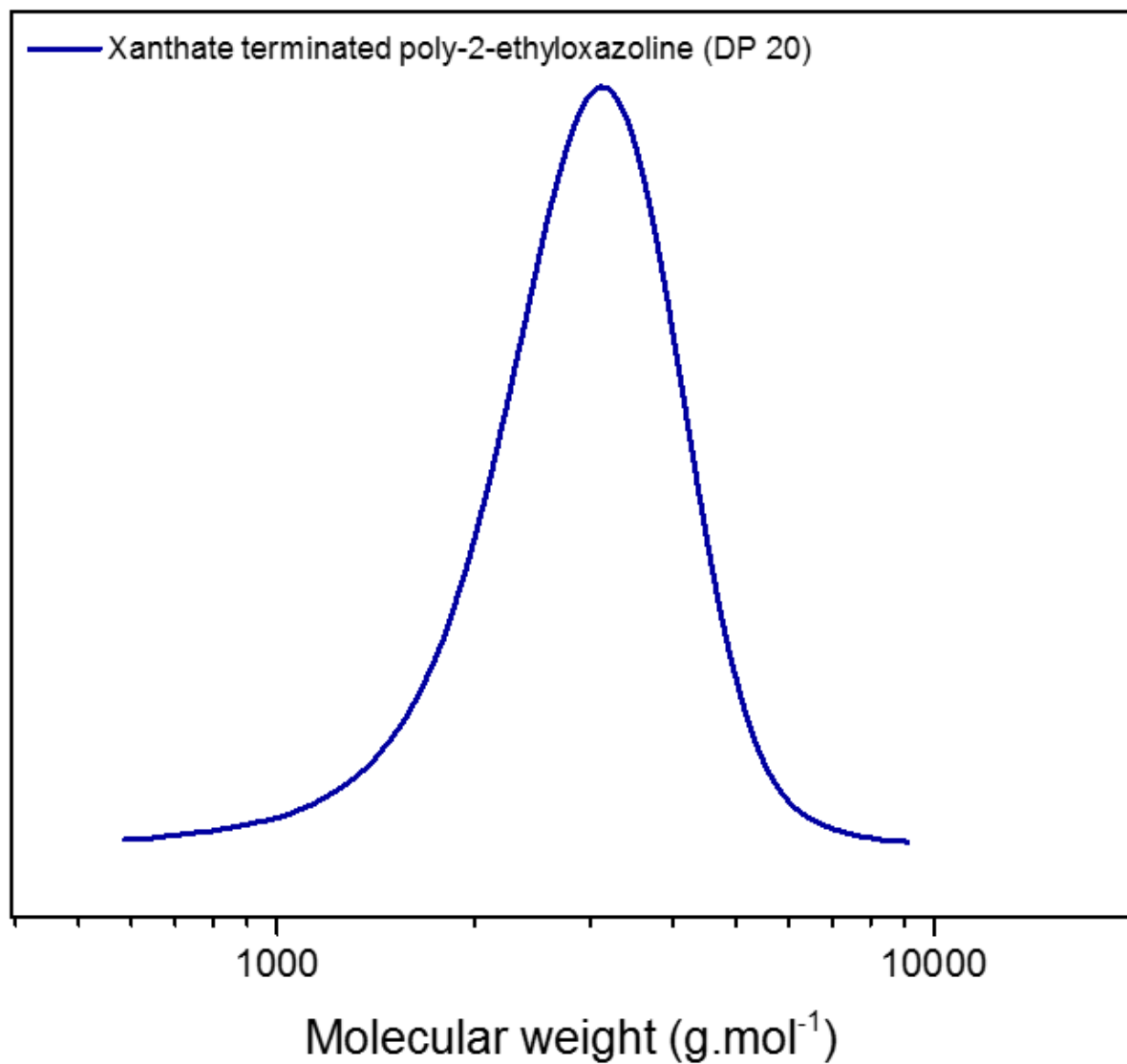


Figure S 4: SEC characterisation of the described poly-2-ethyloxazoline. Measurement was performed in chloroform with 2% trimethylamine additive, a polystyrene calibration was used as described in the Experimental section.